AGU100 ADVANCING EARTH AND SPACE SCIENCE

Water Resources Research

RESEARCH ARTICLE
10.1029/2019WR025863

Role of Extreme Precipitation and Initial Hydrologic Conditions on Floods in Godavari River Basin, India

Shailesh Garg[1] and Vimal Mishra[1]

[1]Civil Engineering, Indian Institute of Technology (IIT) Gandhinagar, Gandhinagar, India

Key Points:
- A statistically significant increase in annual maximum precipitation was observed for the catchments upstream of four gage stations during the 1955-2016 period in Godavari river basin (GRB)
- The rise in annual maximum streamflow during 1955-2016 at all the four gage stations in GRB was not statistically significant
- Probability of floods driven by extreme precipitation (PF_{EP}) varies between 0.55 and 0.7 at the four gage stations of the GRB

Supporting Information:
- Supporting Information S1

Correspondence to:
V. Mishra,
vmishra@iitgn.ac.in

Citation:
Garg, S., & Mishra, V. (2019). Role of extreme precipitation and initial hydrologic conditions on floods in Godavari river basin, India. *Water Resources Research*, *55*, 9191–9210. https://doi.org/10.1029/2019WR025863

Received 26 JUN 2019
Accepted 23 OCT 2019
Accepted article online 8 NOV 2019
Published online 16 NOV 2019

Abstract Floods are the most frequent natural calamity in India. The Godavari river basin (GRB) witnessed several floods in the past 50 years. Notwithstanding the large damage and economic loss, the role of extreme precipitation and antecedent moisture conditions on floods in the GRB remains unexplored. Using the observations and the well-calibrated Variable Infiltration Capacity model, we estimate the changes in the extreme precipitation and floods in the observed (1955–2016) and projected future (2071–2100) climate in the GRB. We evaluate the role of initial hydrologic conditions and extreme precipitation on floods in both observed and projected future climate. We find a statistically significant increase in annual maximum precipitation for the catchments upstream of four gage stations during the 1955–2016 period. However, the rise in annual maximum streamflow at all the four gage stations in GRB was not statistically significant. The probability of floods driven by extreme precipitation (PF_{EP}) varies between 0.55 and 0.7 at the four gage stations of the GRB, which declines with the size of the basins. More than 80% of extreme precipitation events that cause floods occur on wet antecedent moisture conditions at all the four locations in the GRB. The frequency of extreme precipitation events is projected to rise by two folds or more (under RCP 8.5) in the future (2071–2100) at all four locations. However, the increased frequency of floods under the future climate will largely be driven by the substantial rise in the extreme precipitation events rather than wet antecedent moisture conditions.

1. Introduction

India witnessed several floods historically that affected millions of people, caused loss of lives, and damaged infrastructure and agriculture. For instance, the Mumbai flood of 2005 caused by extremely heavy precipitation affected nearly 20 million lives and killed 1,200 people (Gupta & Nair, 2010). In June 2013, multiday heavy precipitation and outburst of glacial lakes caused flooding in Uttarakhand, which resulted in the loss of more than 4,000 lives with an economic loss of about $3.8 billion (Kumar, 2013). Heavy rainfall occurred in December 2015 led to severe flooding in Chennai and led to the estimated damage of $3 billion (Geert Jan van Oldenborgh et al., 2016). Furthermore, in August 2018, Kerala experienced a devastating flood that killed more than 440 people (Mishra, Aaadhar, et al., 2018; Mishra & Shah, 2018) and caused complete disruption of daily life (Gulf News, 2018). The Kerala flood occurred due to multiday heavy precipitation extremes, while the role of the reservoir storage in amplifying the flood remains under scrutiny (Mishra, Aaadhar, et al., 2018; Sudheer et al., 2019).

Floods are considered as the most frequent natural calamity in India, which result in loss of human lives and infrastructure. The areas that receive floods more frequently are located in Brahmaputra and Kosi river basins (Dhar & Nandargi, 2000; Sinha et al., 2008). However, here we mainly focus on flood occurrence in the Godavari river basin (GRB), which has also faced some of the major floods in the past. For instance, the flood in September 1959 in the mainstream Godavari at location Dowlaiswaram and the flood in August 1976 in stream Indravati caused severe damage in the lower reaches of the basin (Rakhecha, 2002). In August 1986, GRB experienced an extreme flood that inundated the downstream regions affecting millions of people and caused a loss of more than 250 lives (Rakhecha & Singh, 2017).

Riverine floods are caused by several factors including extreme precipitation, dam failure, ice and glacier melting, cloudburst, poor reservoir operations, and rain-on-snow events (Cao et al., 2019; Dhar & Nandargi, 2003). However, extreme precipitation is considered one of the most likely factors that cause floods regardless of the topographical characteristics of the basin (Ivancic & Shaw, 2015; Mirza, 2011) particularly in the monsoon dominated climate. Apart from natural drivers, anthropogenic factors such as rapid urbanisation, deforestation, the encroachment of floodplains, poor management of embankments, and

faulty reservoir operations can cause or amplify floods in Indian subcontinental rivers (Bhattachaiyya & Bora, 1997; Dhar & Nandargi, 2003). Heavy precipitation in upstream areas of a river basin makes it challenging to accommodate the high flows in reservoirs that are already full, which causes a sudden release of discharge from reservoirs resulting in flood inundation in the downstream regions (Jena et al., 2014). Failure of dams and other water retaining structures caused some devastating floods in the past. For instance, the sudden collapse of the Machhu dam in August 1979 in Saurashtra caused a loss of more than 10,000 human lives and damage of property and agricultural lands (Dhar et al., 1981).

River basin characteristics (e.g., basin steepness, basin geometry, drainage area, land use land cover, drainage density, and soil moisture conditions) play an essential role in flood generation (Blöschl et al., 2015, 2013; Merz & Blöschl, 2009; Pilgrim et al., 1982). However, antecedent moisture conditions play a significant role in the timing and magnitude of flood events (Berghuijs et al., 2019; Cao et al., 2019; Ivancic & Shaw, 2015; Slater & Wilby, 2017). For instance, extreme precipitation over a drier antecedent condition of catchment while low-intensity multiday precipitation over a catchment with wetter antecedent conditions can result in a flood of comparable magnitude (Cea & Fraga, 2018). In smaller or urban catchments, antecedent soil moisture conditions may not be directly linked with the floods. However, in the larger catchments, antecedent soil moisture or initial hydrologic conditions (IHCs hereafter) can influence streamflow and flood generation significantly (Smith et al., 2013). Therefore, the role of antecedent moisture conditions is considered in the hydrological and rainfall-runoff models (Camici et al., 2011; Massari et al., 2014).

Previous studies reported that the antecedent moisture or IHCs can be a major factor besides extreme precipitation that controls flood generation at river basin scale (Berghuijs et al., 2019; Cao et al., 2019; Ivancic & Shaw, 2015; Li et al., 2009; Radatz et al., 2012; Tramblay et al., 2010). However, none of these studies represents the extreme precipitation driven floods during the monsoon season in India. As there is a consensus that warming climate will increase extreme precipitation events, which have already been increasing in India as well (Roxy et al., 2017). However, the translation from extreme precipitation to floods is not straightforward, especially in the monsoonal climate, which underscores the need for further studies. Flooding in India during the monsoon season has a unique feature—dry soils during the premonsoon (April and May) due to hot summers and extremely wet soils during the mid and end part of the monsoon (June–September). Therefore, the intraseasonal variability of the monsoon and timing of extreme precipitation events in India play a vital role in the occurrence of floods.

The frequency of extreme precipitation and floods are projected to increase under the warming climate in the Indian subcontinent (Mukherjee et al., 2018; Roxy et al., 2017). However, the projected increase in the frequency of extreme precipitation under the warming climate may not proportionally result in the increased frequency of floods (Ali et al., 2019; Ivancic & Shaw, 2015; Sharma et al., 2018). While the increase in extreme precipitation can be directly linked to increased water vapor in the atmosphere in response to climate warming (Ali & Mishra, 2018; Trenberth et al., 2003; Westra et al., 2013), floods may or may not be directly driven by extreme precipitation (Sharma et al., 2018). Notwithstanding the increased occurrence of floods in the current and future climate (Ali et al., 2019; Hirabayashi et al., 2013; Kundzewicz et al., 2014), the role of IHCs and other governing factors on floods in India remains largely unexplored. Here we, for the first time, explore the role of IHCs on floods in the observed and projected future climate in India. We use gridded observations and future projections from Coupled Model Intercomparison Project-5 (CMIP5) general circulation models (GCMs) to estimate the observed and projected changes in the extreme precipitation and floods in the GRB. Our focus here is to evaluate the role of IHCs and extreme precipitation on floods in GRB under the observed and projected future climate. We mainly aim to address the question: To what extent do the initial hydrologic conditions and extreme precipitation influence floods in the GRB in the observed (1951–2016) and projected future climate (2071–2100)?

2. Study Area

The Godavari is the second-longest river in India after the Ganges and the longest among all the rivers in peninsular India with a length of 1,465 km. The Godavari originates from Nasik, Maharashtra, and falls into the Bay of Bengal (East Coast of India). GRB (Figure 1) is located in the central and southern parts of India. GRB has a total drainage area of approximately 312,813 km^2, which is nearly 9.2% of the total geographical area of the country. GRB has a tropical climate where southwest monsoon contributes nearly 85% of the total

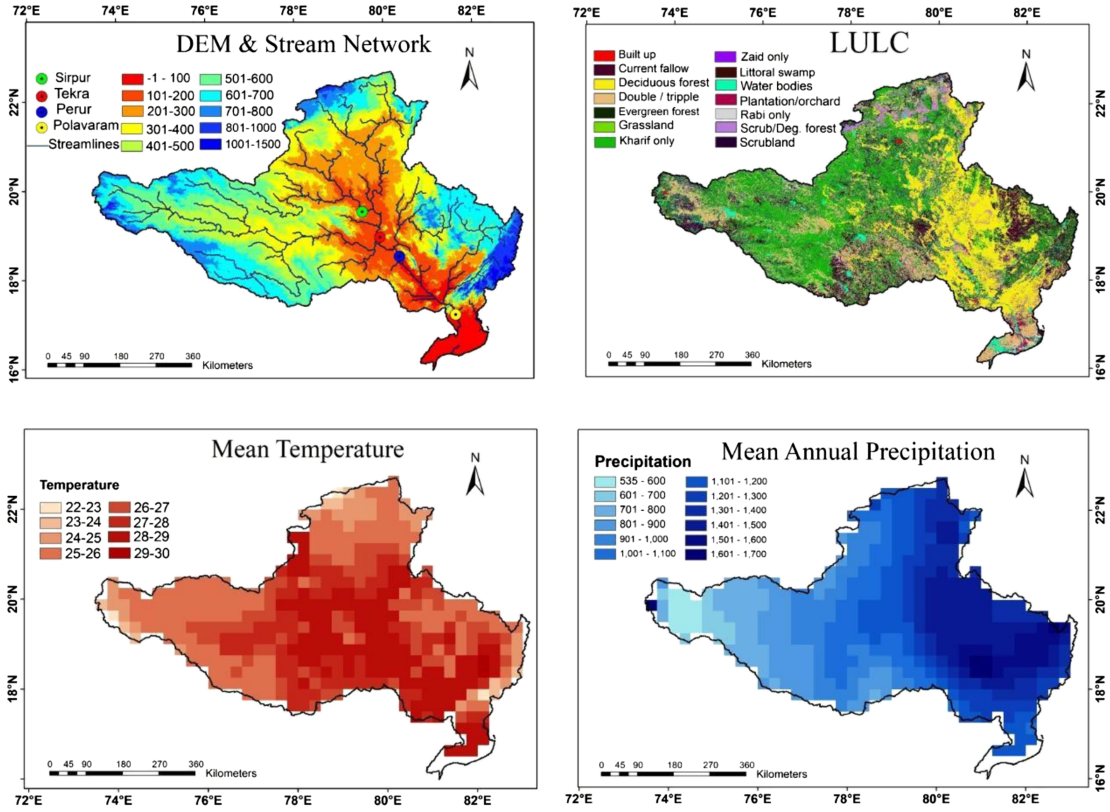

Figure 1. Basic information of Godavari river basin (GRB) including topography, LULC, annual mean precipitation and temperature for the period 1951–2016. DEM = digital elevation model; LULC = land use land cover.

annual rainfall over the basin. The Western Ghats act as an orographic barrier that influences the rainfall patterns in peninsular India (Gunnell et al., 2007). Upper Godavari is characterized by the arid to the semi-arid climate with relatively lesser (500–1,200 mm) mean annual precipitation, while lower Godavari is comparatively moist with higher (1,200–2,000 mm) mean annual precipitation (Asouti & Fuller, 2008). Further details about the GRB characteristics can be seen in Figure 1.

According to the National Disaster Management Authority of India, downstream part of the GRB is prone to floods. Even though Godavari river has adequate capacity to carry the streamflow within the limits of its natural banks, the lower reaches of the stream and some deltaic areas still face numerous floods because of the flatbed slope (Mohapatra & Singh, 2003). During the monsoon season (June to September), Godavari spills its banks in response to extreme precipitation primarily in the lower reaches and in the downstream of the confluence of the river Indravathi with the Godavari. Some areas in Telangana and Andhra Pradesh are the most flood-prone regions in the Godavari basin because the three principal tributaries including Pranahita, Indravathi, and Sabari, drain into it over its last stretch of 473 km. Unfortunately, Telangana and Andhra Pradesh are victims of their topography. Between 1962 and 1990, flood warnings were issued 22 times at Dowlaiswaram (Andhra Pradesh), where the peak discharge exceeded 19,800 m^3/s (Nageswara Rao, 2001). Out of the four selected gage stations that we considered for our analysis in GRB, Sirpur has the smallest subbasin area (48,843 km^2) followed by Tekra (110,079 km^2), Perur (252,963 km^2), and then Polavaram (307,638 km^2). In this study, we present the analysis considering No Irrigation No Dam conditions, and the influence of water management or irrigation was not considered in our simulations.

3. Data and Methods

3.1. Data Sets

We obtained the gridded daily precipitation (mm) for the GRB from India Meteorological Department (IMD) at 0.25° spatial resolution for the period 1951–2016 (Pai et al., 2015). IMD provides climate data for India

from 1901 to the present. IMD collects observations from 6,995 rain gages across the country and uses an inverse distance weighting interpolation scheme (Shepard, 1984) to develop the gridded precipitation products. Similarly, we obtained the gridded daily minimum and maximum air temperature (°C) from IMD for the period 1951–2016. Minimum and maximum temperatures at 1° spatial resolution were developed using the observations from 395 gage stations across the country (Srivastava et al., 2009). We obtained the daily wind speed data from the National Centre for Environmental Prediction/National Centre for Atmospheric Research global reanalysis data set (http://www.cdc.noaa.gov/cdc/data.ncep.reanalysis.surface.html). Daily temperature and wind speed data sets were further regridded to 0.25° using the methodology described in Maurer et al. (2002). We used Shuttle Radar Topographic Mission digital elevation model data at 30-m spatial resolution to extract the topographical features within the GRB (Figure 1). Further, we obtained the daily observed streamflow data from India Water Resources Information System Portal (India-WRIS: http://www.india-wris.nrsc.gov.in). Streamflow data are collected by the Central Water Commission at multiple gage stations across the country. Although streamflow data are available at more than 65 locations in the GRB, the data availability is either short term or intermittent in many places. Therefore, we selected the gage stations based on long-term continuous data availability and the least influence of water management activities as described in Mishra, Shah, et al. (2018) and Shah and Mishra (2016). Therefore, our analysis does not consider the role of human influence and water management activities on floods in GRB. We aim to consider the role of extreme precipitation and IHCs under the natural setting without under any human influence (irrigation, reservoir storage, or water diversion).

To estimate the projected change in climate extremes in the future, we obtained daily climate forcing (precipitation and maximum and minimum temperatures) from five CMIP5-GCMs (Taylor et al., 2012). We selected the five GCMs (BNU-ESM, CESM1-CAM5, GFDL-ESM2M, MPI-ESM-LR, and NorESM1-M) for our analysis as these perform well against the observed key features of the South Asian summer monsoon (Ashfaq et al., 2017). We obtained the climate data for the historical (1951–2005) and future (2006–2100) periods for the three different Representative Concentration Pathways (RCPs): RCP 2.6 (low emission), RCP 4.5 (moderate emission), and RCP 8.5 (high emission) (Moss et al., 2010). Since the GCMs have some bias in the precipitation and temperature, we further downscaled and bias-corrected daily data from CMIP5-GCMs to 0.25° spatial resolution using trend-preserving statistical bias correction approach (Hempel et al., 2013). In this approach, monthly mean and daily variability of model-simulated climate data are adjusted to observations. The long-term trends in the data are preserved.

3.2. The Variable Infiltration Capacity Model

We used Variable Infiltration Capacity (VIC, version 4.1.2) model (Cherkauer et al., 2003; Cherkauer & Lettenmaier, 1999; Liang et al., 1994, 1996), which is a large-scale, semi-distributed hydrologic model that simulates the land surface components of both water and energy budgets within a grid cell. The VIC model considers the subgrid variabilities of topography, soil moisture storage capacity, and vegetation (Gao et al., 2009). Meteorological forcings required to run the VIC model include daily or sub-daily precipitation, minimum temperature, maximum temperature, and wind speed. We used daily meteorological forcings for the observed and projected future climate. In addition, the VIC model requires some additional land surface characteristics such as soil parameters, vegetation properties, and topography (elevation bands). Vegetation parameters were obtained from global land cover information of the Advanced Very High-Resolution Radiometer (AVHRR) available at 1 km as described by Hansen et al. (2000). We developed vegetation parameters for the study domain that includes vegetative compositions of different land use/land cover classes for each grid cell. We obtained vegetation library from the Land Surface Hydrology Group's website (www.hydro.washington.edu) of the University of Washington. We developed the soil parameters using data from the Harmonized World Soil Database (HWSD). Simulations for the observed and projected climate were conducted using the VIC model in full water balance mode and daily time step. Observed meteorological forcing at sub-daily time step is not available in India, we, therefore, decided to use daily time step to run the VIC model. To simulate daily streamflow, a separate stand-alone routing model (Lohmann et al., 1996; Lohmann et al., 1998) was used for routing baseflow and runoff from each grid cell at desired locations in GRB. Routing of the simulated runoff and baseflow was performed using daily fluxes, which does not influence our analysis given the large size of subbasins (where gage stations are located) of GRB.

3.3. Analysis Approach

Our approach to evaluate the role of IHC on floods in GRBs employs three major steps: (i) evaluation of changes in the frequency (number of events per year) of extreme precipitation and streamflow events using 95th and 99th percentile thresholds, (ii) selection of the top 100 independent flood events at each gage station, and (iii) estimation of probability of floods caused by extreme precipitation events and the role of IHCs prior to extreme precipitation based on 7-day averaged soil moisture. These major steps are presented in Figure S1 in the supporting information.

First, we checked the frequency of daily extreme precipitation and floods as the number of events that exceeded the 95th and 99th percentile thresholds during the observed record of 1955–2016. We considered two thresholds to get an idea of the total number of extreme events during the observed record, but finally, the 99th percentile threshold was selected for further analysis. In addition, we estimated basin-averaged annual maximum precipitation and the VIC model-simulated annual maximum streamflow at four gage stations. We analyzed trends in the frequency and annual maximum precipitation/streamflow by using a nonparametric Mann-Kendall trend test (Mann, 1945) and Sen's slope method (Sen, 1968). The nonparametric test provides better estimates of linear trend assuming nonnormality in the data set, and it is less sensitive to the missing data and outliers (Yue et al., 2002). For the future period (2071–2100), we estimated the multimodel ensemble mean annual maximum streamflow and the frequency of extreme precipitation/flood (exceeding 99th percentile). The 99th percentile threshold for both streamflow and precipitation was estimated for the historical reference period of 1971–2000 for each CMIP5-GCM and compared with the threshold values for the future period (2071–2100) for each RCP.

Since we are interested to evaluate the role of IHC on the large floods, we selected the top 100 independent (separated by at least 15 days) streamflow events at each station for the observed period of 1955–2016 (in 61 years) using the VIC-simulated streamflow. Although we began the model simulation from 1951, we analyzed streamflow from 1955 and the initial 4 years were considered as model's spin-up period. To evaluate the influence of IHCs on floods, we analyzed soil moisture and precipitation 0 (the day of the flood) to 4 days prior to the top 100 streamflow events. To do so, we considered the top 30-cm soil moisture from the first soil layer of the VIC model, and moisture at deeper depths was not used to avoid the effect of high persistence in soil moisture at deeper depths (Mishra, Shah, et al., 2018). Here we note that the first-layer soil depth of the VIC model was set to 30 cm, and the second and third-layer depths were calibrated along with other parameters. The second soil layer characterizes the slowly varying soil moisture between the two storms (Liang et al., 1994) and therefore can influence initial hydrologic conditions (Gao et al., 2009). Since we considered the 7-day mean basin averaged soil moisture to analyze initial hydrologic conditions, the overall response from both the layers can be effectively captured by the soil moisture of the top layer. In addition, we evaluated the spatial distribution of IHCs at 0 to 4 days prior to the top three floods that occurred during the observed climate (1955–2016) at each station.

To understand the effect of catchment area on the role of IHCs on the observed floods in GRB, we selected independent (separated by at least 3 days) extreme precipitation events during the observed record of 1955–2016. Basin-averaged precipitation exceeding the 99th percentile of the rainy days (precipitation $\geq$ 1 mm) was considered as extreme precipitation. Since the area contributing to each flood may depend on the orientation of storms within the basin, we assume that basin averaged extreme precipitation and soil moisture can represent the overall conditions and their influence on floods. However, we note that in the regions that receive extreme precipitation can have more influence on the individual flood. To identify the floods caused by extreme precipitation, we estimated the occurrences streamflow exceeding the 99th percentile caused by extreme precipitation events during the 1955–2016 period. If streamflow exceeding the 99th percentile (flood) occurred within 0 to 4 days of the occurrence of extreme precipitation, we considered this flood caused due to extreme precipitation. We repeated this analysis for all the stations based on basin averaged extreme precipitation and floods. This analysis provided us with an idea of the extreme precipitation-driven floods by considering the number of times extreme precipitation events result in floods at the selected gage stations. Moreover, for each station, we estimated the number of extreme precipitation that caused or (did not cause) the flood.

Next, extreme precipitation events were categorized based on the basin averaged soil moisture. Ivancic and Shaw (2015) used basin averaged median soil moisture to identify wet and non-wet conditions. However, to

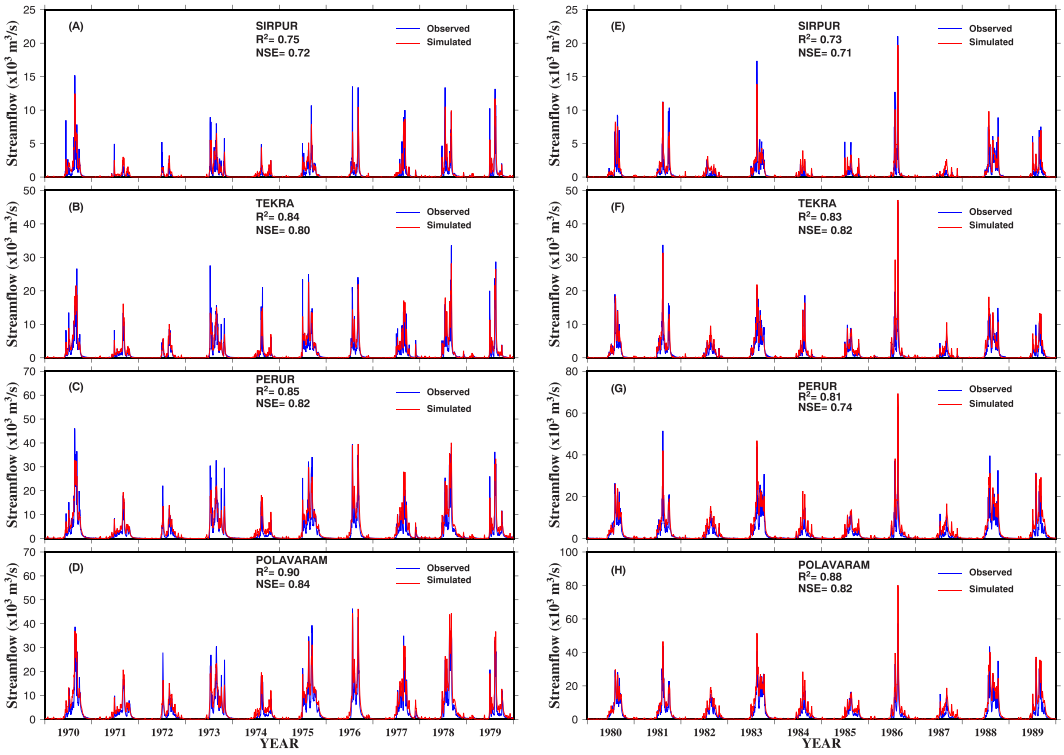

Figure 2. Comparison of daily observed (blue) and the Variable Infiltration Capacity (VIC) model simulated (red) streamflow (m^3/s) for the (a–d) calibration (1970–1979) and (e–h) evaluation (1980–1989) periods at the selected gage stations Sirpur, Tekra, Perur, and Polavaram. Coefficient of determination (R^2) and Nash-Sutcliffe Efficiency (NSE) for the calibration and evaluation periods are provided.

ensure the robust contribution of initial hydrologic conditions, we considered the 75th percentile to effectively cover the basin-averaged moisture conditions and ignore the events that influence only a part of the basin. To do so, we estimated soil moisture 0 to 6 days prior to an extreme precipitation event. We considered 7-day (0–6 days) mean soil moisture prior to an extreme precipitation event in our analysis for the IHCs. Moreover, 7-day mean soil moisture for the same duration was estimated for each year during the period of 1955–2016 to understand if the IHC was drier or wetter. Using these 62 samples (one for each year during 1955–2016) of 7-day mean soil moisture, we fitted the generalized extreme value distribution to obtain the cumulative distribution function (CDF). Any 7-day mean soil moisture having CDF more than 0.75 was considered as "wet" IHC. On the other hand, if CDF of 7-day soil moisture of the extreme precipitation event was less than 0.75, we consider it as "non-wet" IHC of the basin. We repeated this analysis for each extreme precipitation event at each station to categorize the extreme precipitation events that occurred on "wet" IHCs or "non-wet" IHCs. Further, we identified if flood events were caused by the combination of extreme precipitation and wet IHC or extreme precipitation and non-wet IHC. We also identified the extreme precipitation events that did not cause the flood. For these events, we evaluated the IHCs to understand if these occurred in non-wet antecedent moisture conditions. We then estimated the probability of floods driven by extreme precipitation (PF_{EP}) by dividing the number of flood events due to extreme precipitation to a total number of extreme precipitation events.

Next, we estimated the number of events in the future period (2071–2100) that exceeded the 99th percentile precipitation of rainy days in the historical reference period (1971–2000). We compared the frequency of extreme precipitation events for the future and historic periods considering the same 99th percentile threshold. We estimated the number of extreme precipitation events that occurred on the wet IHC (EP_{WIHC}) and compared them with the total number of extreme precipitation events for both historical and future periods. The categorization of the IHCs (wet or not wet) in the historical and future periods for the five CMIP5-GCMs and the three RCPs was based on the cumulative distribution (more than 0.75) of 7-day averaged soil moisture conditions in the historical reference period (1971–2000).

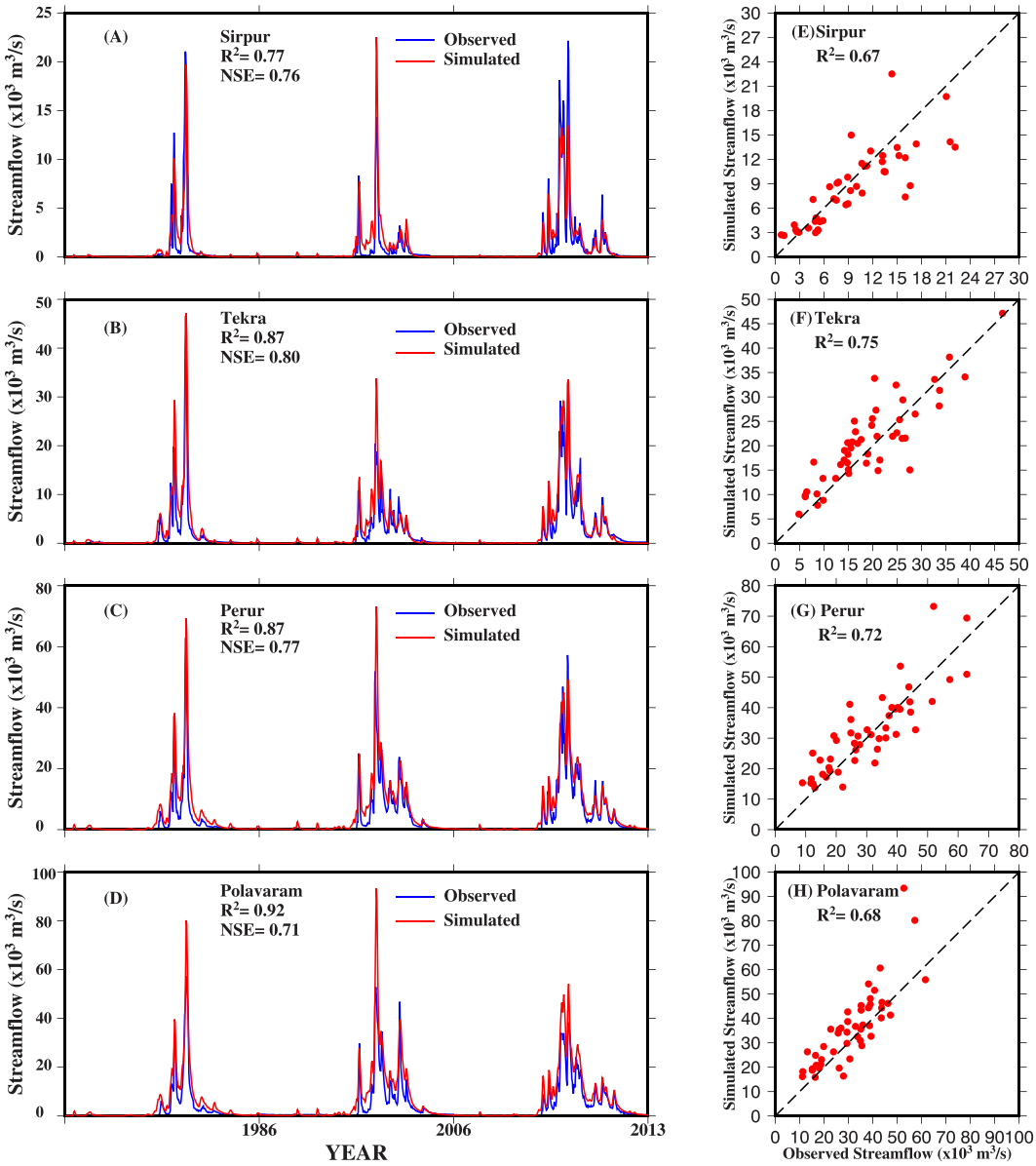

Figure 3. (a–d) Comparison of daily observed (blue) and the Variable Infiltration Capacity (VIC) model simulated (red) streamflow (m^3/s) for the three major flood years of 1986, 2006, and 2013 at Sirpur, Tekra, Perur, and Polavaram. (e–h) The VIC model performance evaluation for simulated annual maximum streamflow against observed annual maximum streamflow for the period 1955–2016 at all the four gage stations. NSE = Nash-Sutcliffe efficiency.

4. Results and Discussion

4.1. Performance of the VIC Model

First, we evaluated the performance of the VIC model at the selected gage station of GRB. We calibrated the VIC model against the observed daily streamflow in GRB at four (Sirpur, Tekra, Perur, and Polavaram) gage stations. We selected these stations based on the criteria that they are not (or least) influenced by the water management activities in the upstream regions. We selected 1970–1979 as the calibration period and 1980–1989 as the evaluation period based on the availability of the observed data at all four stations. Most of the major reservoirs upstream of these basins were constructed after 1985. Therefore, we consider streamflow in the calibration and at least in the major part of the evaluation period is not affected by the major reservoirs.

We estimated Nash-Sutcliffe efficiency (NSE; Nash & Sutcliffe, 1970) and coefficient of determination (R^2) between simulated and observed daily streamflow for the calibration and evaluation periods. The VIC

Table 1
The Performance of the VIC Model for the Calibration, for the Evaluation Periods, and for the Three Selected Flood Years (1986, 2006, and 2013)

	Calibration period 1970–1979		Evaluation (Validation) period 1980–1989		Year 1986, 2006, and 2013	
Stations	R^2	NSE	R^2	NSE	R^2	NSE
Sirpur	0.75	0.72	0.73	0.71	0.77	0.76
Tekra	0.84	0.80	0.83	0.82	0.87	0.8
Perur	0.85	0.82	0.81	0.74	0.87	0.77
Polavaram	0.90	0.84	0.88	0.82	0.92	0.71

model performed well (Moriasi et al., 2007) to simulate daily streamflow with NSE and R^2 more than 0.70 at all four locations for both calibration and evaluation periods (Figure 2).

Since we mainly focus on the floods in GRB, we analyzed the performance of the VIC model for the three (1986, 2006, and 2013) major flood events in GRB. We find that the VIC model-simulated streamflow compares well against the observed flow for the major floods with NSE and R^2 more than 0.70 at all the stations (Figure 3). Further, we evaluated the performance of the VIC model for annual maximum streamflow at four stations in the basin. We note that the VIC model satisfactorily captures the observed annual maximum flow at all four gage stations with R^2 higher than 0.65 (Figure 3). Overall, the VIC model performed well and successfully captured temporal variability and peaks in daily streamflow at all four gage stations in GRB. Since the VIC model has been evaluated for other hydrologic variables (evapotranspiration and soil moisture) in India in the previous studies (Shah et al., 2019; Shah & Mishra, 2016), we limit our evaluation to daily streamflow and flood events. A detailed assessment of the VIC model performance at four gage stations in GRB is presented in Table 1. Overall, we find that our well-calibrated and evaluated setup of the VIC model can be used to evaluate the role of IHCs and extreme precipitation on floods in GRB under the observed and projected future climate. Here we consider the natural scenario and any influence of human activities (such as irrigation, water diversion, and reservoirs) was not simulated.

4.2. Observed Precipitation Extremes and Floods, 1955–2016

Next, we evaluate the changes in annual maximum daily streamflow and annual maximum precipitation for the observational period of 1955–2016 at each gage station. Annual maximum precipitation was estimated using averaged daily precipitation for the basins upstream of the gage stations. We find the annual maximum precipitation has increased significantly ($p$value < 0.05) during 1955–2016 (Figure 4). The highest increase in annual maximum precipitation during the observational record was experienced in the catchments of Sirpur, followed by Tekra, Perur, and Polavaram. Increase in extreme precipitation in India has been reported in many previous studies (Goswami et al., 2006; Mukherjee et al., 2018; Roxy et al., 2017). For instance, Roxy et al. (2017) reported that extreme precipitation has increased three folds in central India during the last few decades. The observed increase in extreme precipitation can be associated with the recent warming that has contributed to an increase in atmospheric water vapor (Ali & Mishra, 2017). Moreover, both thermodynamical (localized) and dynamical (large-scale) components can contribute to the increase in extreme precipitation under the current and future climate in India (Ali & Mishra, 2018; Roxy et al., 2017). Overall, we find that the upstream catchments of all the gage stations experienced a significant rise in annual maximum precipitation during 1955–2016.

We expected that the significant increase in the extreme precipitation in the upstream basins of four stations would translate into increased annual maximum streamflow. However, the increase in annual maximum streamflow at any of the four stations is not statistically ($p$value more than 0.05) significant (Figure 4). Further, the increase in precipitation extremes in the basin is not directly related to the increase in streamflow at the basin outlet, which is attributable to catchment characteristics and antecedent moisture conditions (Berghuijs et al., 2019; Saharia et al., 2017). For instance, Sharma et al. (2018) reported that the changes in precipitation are not directly linked to flooding because of the other dominating factors.

In addition to annual maximum precipitation and streamflow, we estimated the frequency of precipitation and the VIC model-simulated streamflow exceeding of 99th and 95th percentiles of the observed (1955–

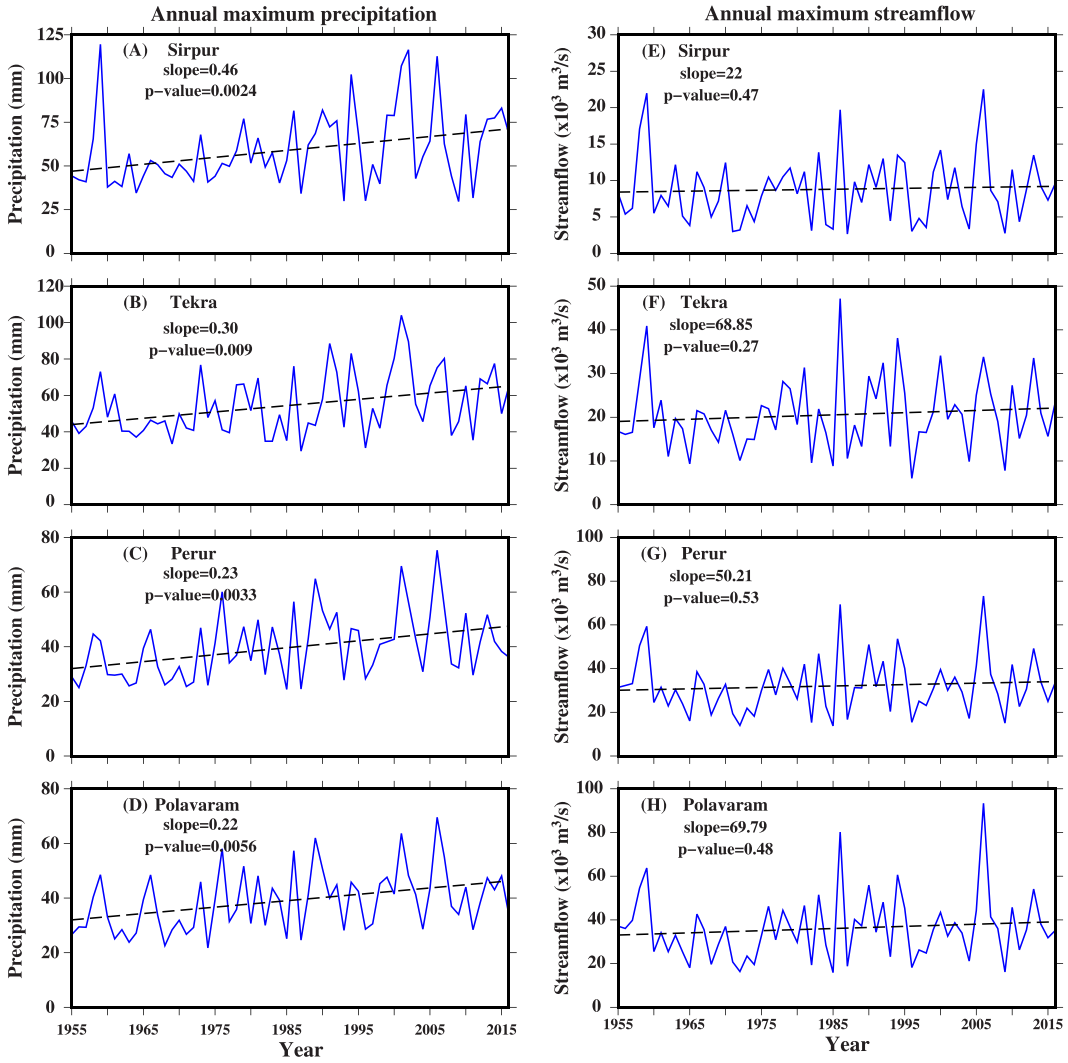

Figure 4. (a–d) annual maximum precipitation and (e–h) the Variable Infiltration Capacity (VIC) model simulated annual maximum streamflow for the observed period 1955–2016 at the four gage stations Sirpur, Tekra, Perur, and Polavaram in the GRB. Dotted lines represent the fitted linear trend estimated using the nonparametric Mann-Kendall test and Sen's slope (mm/year) method. Annual maximum precipitation was estimated using basin-averaged precipitation for the catchments located upstream of the four gage stations; *p*value less than 0.05 shows statistically significant trend at 5% significance level.

2016) period. We find that the frequency of extreme precipitation and streamflow has increased during the observed record (1955–2016) in the GRB (Figure 5). While the frequency of extreme precipitation has significantly ($p$value < 0.05) increased for the basin upstream of Perur and Polavaram, the rising trend in the frequency of extreme discharge was not found significant at any streamflow gage stations (Figure 5). In addition, we evaluated the changes in the frequency of extreme precipitation and streamflow exceeding the 95th percentile (Figure S2). However, trends were not found statistically significant. Deshpande et al. (2016) reported that the intensity of heavy precipitation events and the area experiencing extreme precipitation had increased significantly in the GRB in the past few decades. Moreover, Kale (2012) also found a nonsignificant increase in annual maximum streamflow at the Dowlaiswaram station in the lower GRB. The contrast between changes in annual maximum precipitation and streamflow highlights the role of initial hydrologic conditions or other basin characteristics on floods in GRB.

4.3. Role of IHCs on Observed Floods

To understand the role of IHC, we evaluated precipitation and soil moisture conditions for the top hundred independent streamflow events at the four gage stations. For each of these streamflow events, we analyzed

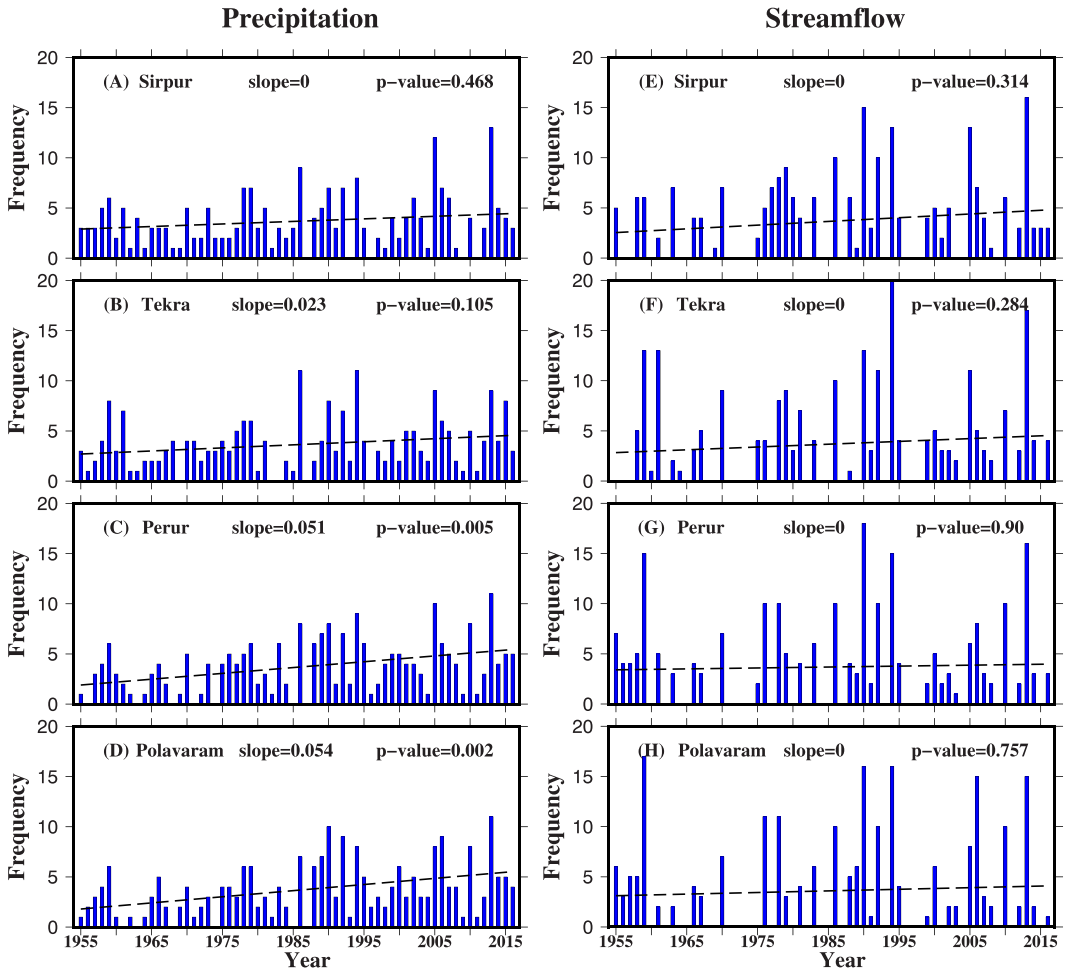

Figure 5. The frequency of extreme precipitation events exceeding 99th percentile of the observed period (a–d) and (e–h) daily streamflow events exceeding 99th percentile computed using the daily at Sirpur, Tekra, Perur, and Polavaram. Dotted lines represent the fitted linear trend in the frequency of extreme precipitation and streamflow using the nonparametric Mann–Kendall test and Sen's slope (events/year) method. Statistical significance was tested at 5% significance level. P-value less than 0.05 shows a statistically significant trend at 5% significance level.

precipitation and soil moisture at 30-cm depth (the first soil layer of the VIC model) from the day of flood to 4 days prior (0 to -4 days of the flood event considering the day of flood as 0). We constructed empirical CDF of precipitation and soil moisture of the top 100 events (Figure S3). Our results show that precipitation and soil moisture are the highest on second (-2) and third (-3) days prior to the flood event for the three (Sirpur, Tekra, and Perur) out of four stations (Figure S3). On the other hand, precipitation and soil moisture are the highest on the third and fourth days prior to the flood event at Polavaram station. Therefore, IHCs at 2 and 3 days prior to the flood events contribute to flooding in GRB. Moreover, we find that two-days prior IHCs are more closely linked with the floods in the relatively smaller catchments, while three-days prior IHCs are more closely linked in the large catchments of Polavaram (Figure S3). To evaluate this further, we analyzed the spatial distribution of antecedent precipitation (Figures S4–S7) and soil moisture conditions (Figures S8–S11) of 1–4 days prior to the top three flood events occurred during 1955–2016 at each gage station. Our results further confirm that IHCs 2 and 3 days prior to flood events are most strongly coupled with the floods in the GRB.

Next, we estimated the probability of floods driven by extreme precipitation (PF_{EP}) by taking the ratio of extreme precipitation driven floods and the total number of extreme precipitation events at each station (Figure 6). We find the highest PF_{EP} at Sirpur, followed by Tekra, Perur, and Polavaram. For instance, out of 57 extreme precipitation events in the basin upstream to Sirpur, 40 of them caused floods (Figure 6). Therefore, PF_{EP} at Sirpur is 0.7 during the period of 1955–2016. Moreover, PF_{EP} of 0.62, 0.58, and 0.55

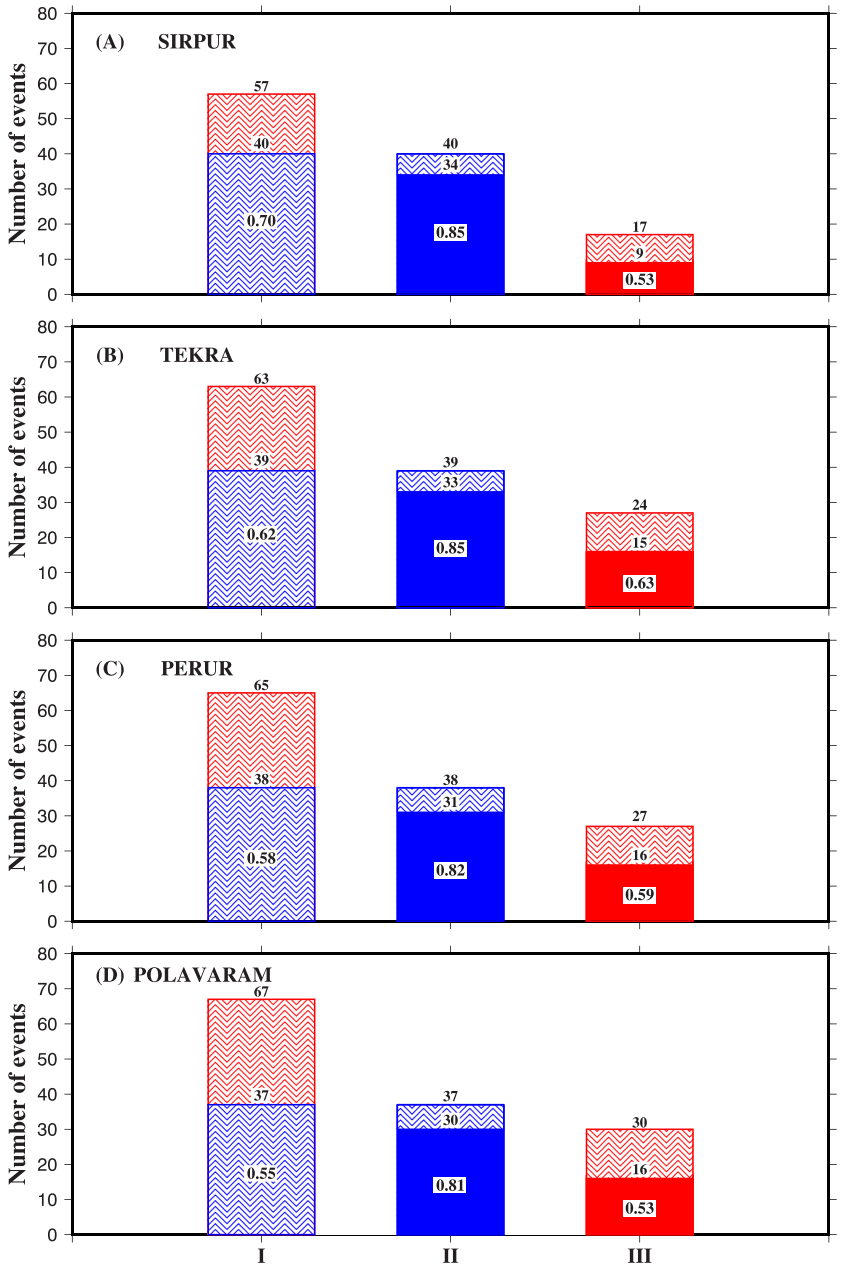

Figure 6. Probability analysis of extreme precipitation events in Godavari river basin for the 1955–2016 period for four stations. (I) Number of extreme precipitation events that caused flood (shaded blue) and did not cause flood (shaded red) out of the total number of extreme events at Sirpur (a), Tekra (b), Perur (c), and Polavaram (d). (II) Number of extreme precipitation events that caused flood with wet soil moisture conditions/IHC (solid blue). (III) Number of extreme precipitation events that did not cause flood with non-wet soil moisture conditions/IHC (solid red). Numbers in (I) represent total number of extreme precipitation events (57), extreme precipitation events that caused floods (40), and the ratio (probability) [40/57: 0.70]. In (II) numbers represent the precipitation events that caused flood (40), extreme precipitation events that occurred on wet IHC (34), and probability (34/40: 0.85). In (III) number of extreme precipitation events that did not cause floods (17), number of extreme precipitation events that occurred on non-wet IHC (9), and probability (9/17: 0.53). Similarly, the values were estimated for the other three stations in (b–d). IHC = initial hydrologic condition.

was found for Tekra, Perur, and Polavaram. Our results indicate the PF_{EP} declines as the size of the river basin increases, which might be associated with the spatial distribution of extreme precipitation in the basin. For instance, in the larger basins, the likelihood is that only a fraction of basin may receive extreme precipitation at a given day and, depending on the flood-producing area, flood peak may get attenuated with a long time of concentration.

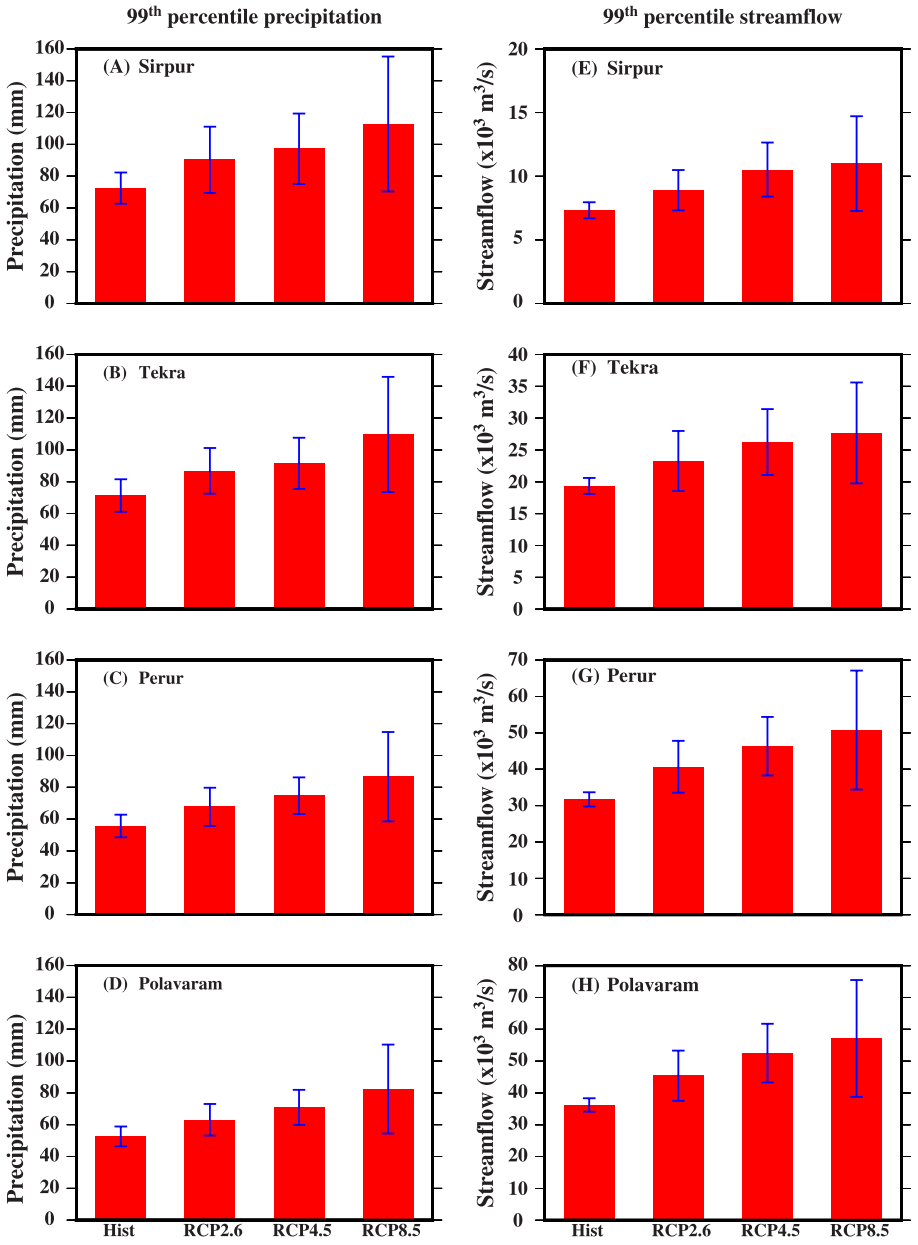

Figure 7. Comparison of multimodel ensemble mean of 99th percentile precipitation and 99th percentile streamflow for the historic (1971–2000) and future (2071–2100) periods based on the RCPs 2.6, 4.5, and 8.5 at (a) Sirpur, (b) Tekra, (c) Perur, and (d) Polavaram. (e–h) same as (a–d) but for 99th percentile of streamflow. Error bars represent the standard deviation for each model-ensemble mean value; 99th percentile precipitation and streamflow were estimated for each general circulation model and Representative Concentration Pathway (RCP), and then the multimodel ensemble mean was taken.

Next, we evaluated the role of IHC on the flood events caused by extreme precipitation. For instance, at Sirpur, out of 57 extreme precipitation events 40 caused floods. Now, we are interested to examine the IHCs prior to these 40 flood events. Our hypothesis is that most of these events are caused by wet IHC prior to an extreme precipitation event. Please note that IHC here is based on 7-days (0, -1, -2, -3, -4, -5, and -6 of the day of extreme precipitation) mean soil moisture. We find that 85% of extreme precipitation that resulted in flood at Sirpur occurred on wet IHC (Figure S12). Similarly, our results show that the combination of extreme precipitation and wet IHC causes flood more than 80% at all the four gage stations of GRB (Figure 6). Here also we note a moderate decline in the role of IHC on flooding for large basins. We further evaluated the IHC prior to extreme precipitation events that did not cause a flood in the GRB (Figure 6). For instance, 17 extreme precipitation events (out of 57) did not result in floods at Sirpur. Therefore, we

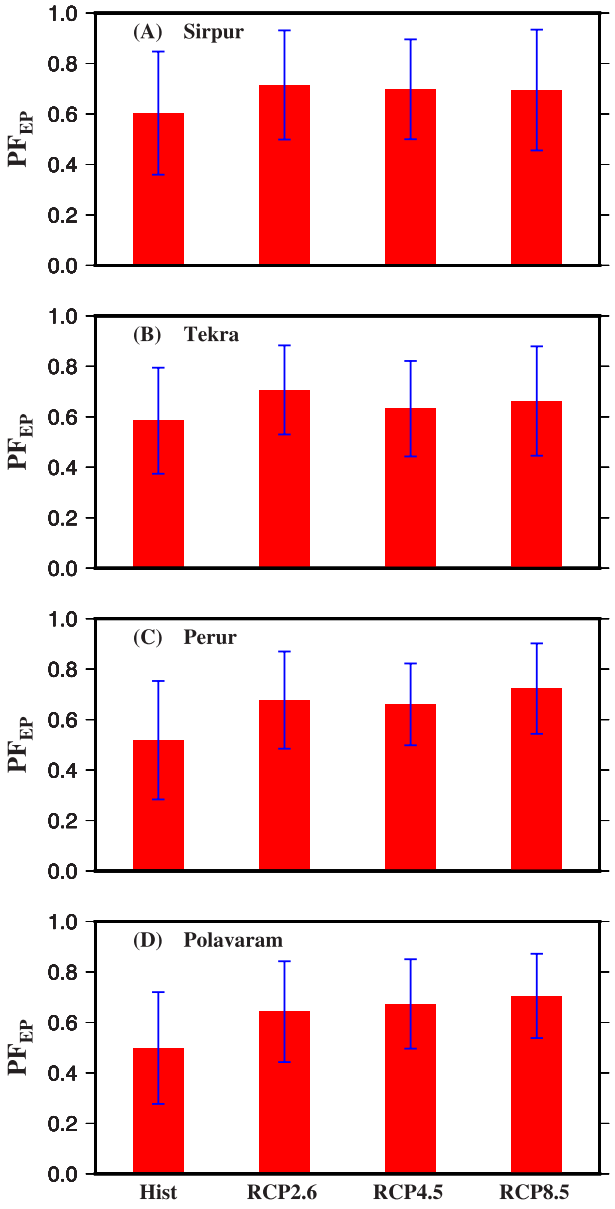

Figure 8. Multimodel ensemble mean of flood probabilities driven by extreme precipitation (PF_{EP}) for the historic (1971–2000) and future (2071–2100) periods under RCP 2.6, RCP 4.5, and RCP 8.5 at (a) Sirpur, (b) Tekra, (c) Perur, and (d) Polavaram. Error bars represent one standard deviation for values from the five general circulation models. RCP = Representative Concentration Pathway.

hypothesize that a majority of these extreme precipitation events might have occurred on non-wet IHC. Our results show that 9 out of the 17 extreme precipitation events that occurred without causing floods were due to non-wet IHC at Sirpur. Similarly, we find that more than 50% of the time combination of nonwet IHC and extreme precipitation will not cause flooding (Figure 6).

After evaluating PF_{EP} at four stations, we extended the analysis and evaluated the PF_{EP} at 19 stations with varying size of their upstream catchments in GRB (Figure S12 and Table S1). We find that while there is a large variability in PF_{EP} of smaller catchments, there is a general trend suggesting a decline in PF_{EP} with the increase in the size of the basin. This large variability in PF_{EP} for the smaller catchments can be attributed to the factors that are not linked with IHCs. There are other dominating factors associated with the basin's topographical and geomorphological characteristics that can dominate over IHC in response to extreme precipitation (Saharia et al., 2017). For instance, the catchments with high slope and drainage density can respond faster to produce floods in response to extreme precipitation. It is noteworthy that in 19 stations located in the GRB, a majority of the floods were caused by the combination of extreme precipitation and wet IHC (Table S1). Similarly, most of the extreme precipitation events that did not cause floods occurred on non-wet IHC in there 19 subbasins of GRB in the observation period 1955–2016. Results show that flooding in the larger basins is more often dependent on the IHCs. Hence, one would not expect that the increased extreme precipitation to will directly influence the occurrence and extent of flooding as noted in the previous studies conducted in the other parts of the world (Berghuijs et al., 2019; Cao et al., 2019; Ivancic & Shaw, 2015; Li et al., 2009; Radatz et al., 2012; Tramblay et al., 2010).

To understand if the extreme precipitation events with higher magnitudes have a high probability of causing floods in the Godavari basin, we divided the extreme precipitations into six bins after sorting them based on their magnitude (from smallest to highest; Figure S13). For the extreme precipitation events in each bin, we estimated PF_{EP}. Our hypothesis here was that extreme precipitation with higher magnitude is more likely to produce flood regardless of IHC and basin size. We find that at all the four stations, there is a general increase in PF_{EP} with the magnitude of extreme precipitation, which indicates that extreme precipitation with high magnitudes is more likely to cause floods. We note that the role of IHCs for extremely heavy precipitation may not be that influential in comparison to the events with less magnitudes. Smith et al. (2013) considered the extreme precipitation as a major factor in the occurrence of flood and reported that the extremely heavy precipitation with thunderstorms is an important factor that influences the upper tail of flood peaks.

4.4. Impacts of Projected Future Climate on Floods

After the assessment of the role of IHCs on floods in GRB during the observed climate (1955–2016), we evaluated the role IHCs on flood in the projected future climate in GRB. We conducted the simulations using the VIC model for the future climate. Before applying the VIC model for the projected future climate, we evaluated the effectiveness of the bias-corrected climate projections for the historical reference period of 1966–2005 for five CMIP5-GCMs (BNU-ESM, CESM1-CAM5, GFDL-ESM 2M, MPI-ESM-LR, and NorESM1-M). As expected, the bias in CMIP5-GCMs in precipitation and temperature was significantly improved after the bias correction (Figures S14 and S15).

Table 2
Multimodel Ensemble Mean of the Probability of Floods Driven by Extreme Precipitation (PF_{EP}) for the Historic (1971–2000) and Future Periods (2071–2100)

Stations		Historic	RCP 2.6	RCP 4.5	RCP 8.5
SIRPUR	Mean	0.60	0.71	0.70	0.69
	Std. deviation	0.24	0.22	0.20	0.24
TEKRA	Mean	0.58	0.71	0.63	0.66
	Std. deviation	0.21	0.18	0.19	0.22
PERUR	Mean	0.52	0.68	0.66	0.72
	Std. deviation	0.23	0.19	0.16	0.18
POLAVARAM	Mean	0.50	0.64	0.67	0.70
	Std. deviation	0.22	0.20	0.18	0.17

Note. RCP = Representative Concentration Pathway.

To estimate the projected changes in the precipitation extremes and floods in the future, we forced the VIC model with bias-corrected daily meteorological forcing from the five CMIP5-GCMs and for the three RCPs (RCPs 2.6, 4.5, and 8.5). The RCPs 2.6 and 8.5 represent the lowest and highest emission scenarios, respectively, and the differences in these two scenarios indicate the impacts of climate change mitigation on extreme precipitation and flood events. We estimated the 99th percentile of precipitation for rainy days for each GCM for the historical (1971–2000) and projected future climate (2071–2100; Figure 7). Similarly, using the VIC model-simulated streamflow at each station, we estimated 99th percentile streamflow for the historical and projected periods. We find that both 99th percentiles of precipitation and streamflow are projected to increase significantly at all four stations under the projected future climate (Figure 7). Moreover, the increase in extreme precipitation and streamflow are substantially higher under the high emission scenario of RCP 8.5 in comparison to the low-emission scenario of 2.6. Therefore, the frequency of extreme precipitation and flood events can be substantially lowered by following the low emission pathway of RCP 2.6. Our results, therefore, highlight the benefits of climate mitigation on the occurrence of extreme precipitation and flood events in the GRB.

Annual maximum streamflow is projected to increase at all the stations of the GRB regardless of the emission scenario (Figure S16). However, the rise in annual maximum streamflow is higher for the high emission scenario of RCP 8.5. Similarly, the warming climate will result in an increased frequency of streamflow events exceeding the 99th percentile (of the 1971–2000 period). We note that the rise in the frequency of foods at all the four stations is higher for the RCPs 4.5 and 8.5 in comparison to RCP 2.6, which again shows that climate change mitigation can reduce the flood risk in the basin (Figure S17). Our results based on the well-calibrated and evaluated model and bias-corrected and downscaled climate projections suggest that there is a robust increase in the magnitude and frequency of extreme precipitation and flood events under the warming climate in Godavari basin.

4.5. Role of IHCs on Projected Floods

Next, we estimated PF_{EP} for all the fifteen combinations (five GCMs and three RCPs) at the four gage stations for the historic (1971–2000) and projected future (2071–2100) periods using the same methodology that was used for the observed climate (1955–2016). First, we estimated PF_{EP} for each GCMs/RCPs at each station and then multimodel ensemble mean PF_{EP} was estimated for the historical and projected future climate. We find that all four stations follow the same trend of a decline in PF_{EP} with an increase in catchment size for the historic period. Moreover, notwithstanding a large intermodel variation, PF_{EP} is projected to increase under the future climate in comparison to the historical period at all the four gage stations of GRB. Furthermore, for the larger basins, the projected increase in PF_{EP} under the high emission scenario of RCP 8.5 is higher than the low emission scenario of 2.6 (Figure 8 and Table 2).

Further, we evaluated the number of extreme precipitation events in the future period (2071–2100) that exceeded the 99th percentile precipitation of historical period (1971–2000) for each GCM and compared them with the number of events exceeded in the historical period for the same precipitation threshold (99th percentile of days with precipitation $\geq$ 1 mm) value. We find an increase in the extreme precipitation events for all the three emission scenarios (Figure 9 and Table 3). The highest increase in the frequency of extreme precipitation events was observed under the RCP 8.5, followed by RCP 4.5 and RCP 2.6. Our results show that by the end of the 21st century (2071–2100) the frequency of extreme precipitation and floods is projected to rise by two folds or more at all the four locations in Godavari basin (Figure 9 and Table 3). The difference in the rise in the frequency of extreme precipitation events under the high (RCP 8.5) and low (RCP 2.6) shows the potential benefits of climate change mitigation (Ali et al., 2019).

IHC plays an important role in floods caused by extreme precipitation events during the observed climate (1955–2016). We further examined the changes in IHCs for all the extreme precipitation events in the historical (1971–2000) and projected future climate (2071–2100). Here our aim is to diagnose if the increased probability of floods under the warming climate in the GRB is driven by the changes in the frequency of

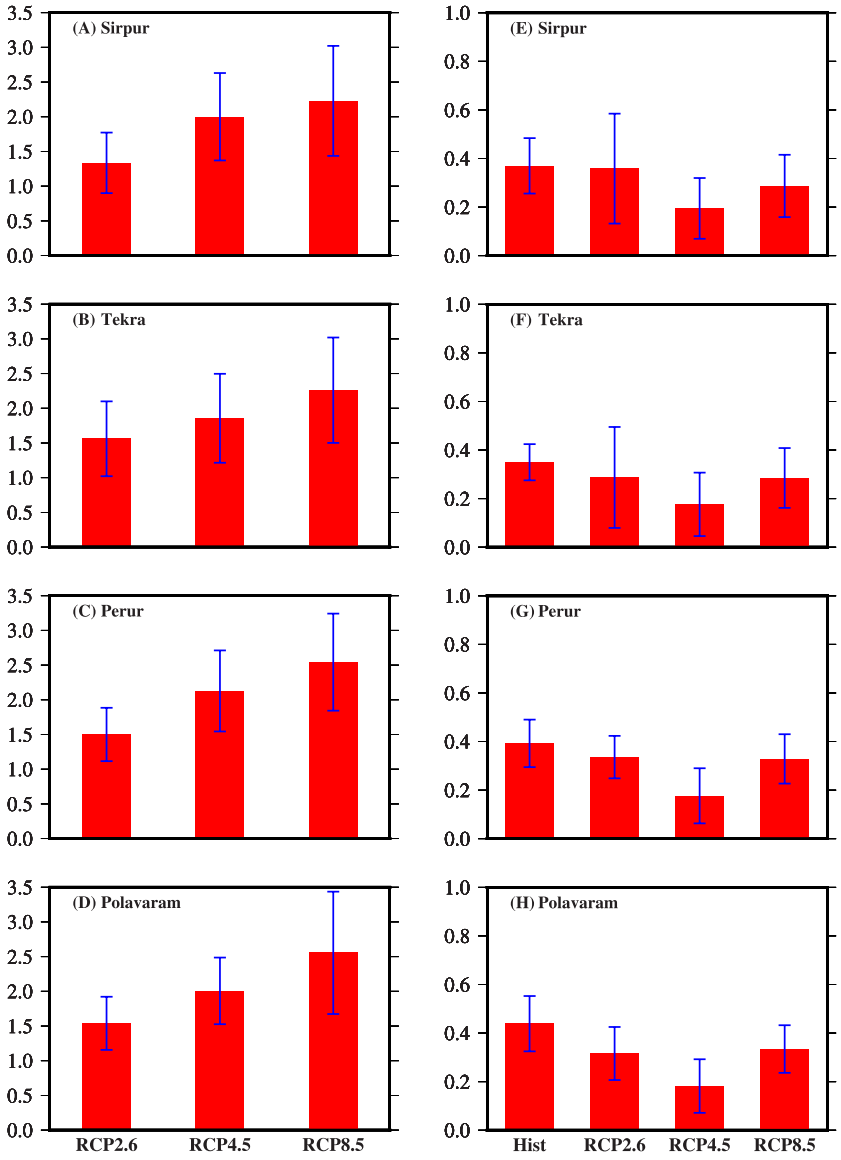

Figure 9. (a–d) Multimodel ensemble mean ratio of number of extreme precipitation events in future (2071–2100) period to the historical (1971–2000) period that exceeded the 99th percentile precipitation of historical period for the three Representative Concentration Pathways (RCPs). (e–h) Multimodel ensemble mean ratio of extreme precipitation occurred on wet initial hydrologic condition in the historic and future periods to the total number of extreme precipitation events for the historical and future periods for the three RCPs at Sirpur, Tekra, Perur, and Polavaram. Error bars represent one standard deviation for values from the five general circulation models.

extreme precipitation events or changes in IHCs. To do so, we compared the extreme precipitation events that occurred on wet IHC (EP_{WIHC}) by taking the ratio of the number of extreme precipitation events that occurred on wet IHC and the total number of extreme precipitation events for the historical and future periods. Wet or non-wet IHCs in both historical and future periods were identified using the cumulative distribution of 7-days averaged soil moisture (0–6 days from the day of extreme precipitation) of the historic period. The increase in the probability of floods caused by extreme precipitation is mainly associated with the increased frequency of extreme precipitation events instead of the increase in the wet IHCs, which can be associated with the interstorm duration under the projected future climate (Figure 9). For instance, if the interstorm duration is less, the IHCs may not play a considerable role in floods.

Table 3
Multimodel Ensemble Mean Ratio of Number of Extreme Precipitation/Flood Events in the Future Period (2071–2100) to the Historical Period (1971–2000) That Exceeded the 99th Percentile Precipitation/Streamflow of Historical Period (1971–2000) for Three Representative Concentration Pathways (RCPs) at Four Gage Stations in the Godavari River Basin

Stations		RCP 2.6	RCP 4.5	RCP 8.5
SIRPUR	Extreme precipitation	1.34	2.00	2.23
	Floods	1.43	1.86	1.78
TEKRA	Extreme precipitation	1.56	1.86	2.26
	Floods	1.46	1.87	1.73
PERUR	Extreme precipitation	1.50	2.13	2.54
	Floods	1.70	2.26	2.19
POLAVARAM	Extreme precipitation	1.54	2.01	2.56
	Floods	1.71	2.27	2.23

Apart from the multimodel ensemble mean changes in PF_{EP}, we also evaluated the changes in each GCMs at the four gage stations of GRB. We find that among the five GCMs, GFDL-ESM 2M and CESM1-CAM5 show higher PF_{EP}, while MPI-ESM-LR, NorESM1-M, and BNU-ESM show relatively lower values of PF_{EP}. To further diagnose this intermodel variability among the five GCMs, we compared basin averaged extreme precipitation (more than the 99th percentile of rainy days) in the five GCMs for historical and future periods. We estimated the kernel density (Terrell & Scott, 1992) at each station for each combination of GCMs and RCP. Our results show that kernel density for GFDL-ESM 2M and CESM1-CAM5 for extreme precipitation is higher, whereas kernel density for MPI-ESM-LR, NorESM1-M, and BNU-ESM is lower (Figure S18). We find that GFDL-ESM 2M and CESM1-CAM5 produce much higher extreme precipitation in comparison to the other GCMs. Therefore, PF_{EP} is higher for these two GCMs. These results are consistent with our observational analysis that shows that PF_{EP} increases with the increase in the magnitude of extreme precipitation. Therefore, our results show that the risk of flooding in GRB is projected to increase due to an increase in the frequency and magnitude of extreme precipitation. Moreover, the increased frequency of floods under that projected future climate will be mainly due to the rise in the frequency of extreme precipitation instead of wet IHCs.

5. Discussion and Conclusions

The frequency and intensity of extreme precipitation have increased in response to the warming climate in many parts of the world (Min et al., 2011; Mishra et al., 2012; Westra et al., 2013). The rise in extreme precipitation in the warming climate is directly linked with the rise in atmospheric water vapor, which can be explained by the Clausius-Clayperon relationship (Ali & Mishra, 2018; Trenberth et al., 2003; Wasko & Sharma, 2015). The flood risk is projected to increase in the future climate globally (Ali et al., 2019; Arnell & Gosling, 2016; Hirabayashi et al., 2013; Milly et al., 2002). However, changes in floods and extreme precipitation may not be directly linked due to the role of land surface characteristics. We find that at the four locations of the GRB, only 50–70% of extreme precipitation events result in floods. While our findings are limited to the four locations in GRB, Wasko and Sharma (2017) estimated the sensitivity of extreme precipitation and streamflow at a global scale and reported that an increase in extreme precipitation does not result in a similar increase in streamflow. We find that more than 80% of extreme precipitation events that caused floods in GRB occurred on wet initial hydrologic conditions. Moreover, initial hydrologic conditions play a relatively lesser role on floods for the smaller basins as we observed at Sirpur in GRB. Consistent with our findings, Wasko and Sharma (2017) also reported that initial hydrologic conditions might become less relevant in increased extreme precipitation and reduced basin size cases. Similarly, Berghuijs et al. (2019), based on the analysis conducted in many catchments in Europe, reported that relatively few annual flood peaks were caused by annual maximum precipitation. In our study, we only considered daily extreme precipitation and floods. Moreover, antecedent moisture conditions were also based on daily soil moisture estimates in GRB. In smaller basins, sub-daily precipitation extremes and antecedent moisture conditions can play a major role in floods. For instance, Cao et al. (2019) reported that storm runoff-precipitation ratio increases with

prestorm wetter conditions. They (Cao et al., 2019) also reported that the role of initial moisture conditions is stronger for the larger catchments, which is consistent with our findings.

We estimated the projected changes in floods and extreme precipitation at the four locations of GRB using downscaled and bias-corrected data from CMIP5-GCMs. The role of the initial hydrologic condition and extreme precipitation may not be static under the changing climatic conditions. This is mainly because of the rise in extreme precipitation frequency and intensity under the warming climate, which is also shown by our results based on the projections from CMIP5-GCMs. Moreover, precipitation characteristics (Asoka et al., 2018) associated with the number of rainy days and distribution of precipitation during the monsoon season may change in the future, which can result in the changes in initial hydrologic conditions. The projections of flooding are uncertain due to the combined effect of changing IHCs and extreme precipitation in the future climate (Kundzewicz et al., 2014). We find that both extreme precipitation events and floods are projected to increase in GRB. However, the projected changes in extreme precipitation and floods vary with the locations as well as emission scenarios. We find that the increased frequency of floods in the future climate is largely contributed by the rise in extreme precipitation events in GRB.

Based on our findings, the following conclusions can be made:

1. Annual maximum precipitation has significantly increased in the catchments upstream of the four gage stations in the GRB during the period of 1955–2016. However, the increase in annual maximum streamflow was not statistically significant at any of four locations, indicating that an increase in extreme precipitation does not directly translate into the rise in annual maximum streamflow. The disparity in the changes in annual maximum extreme precipitation and streamflow are attributable to the role of land surface (catchment characteristics and antecedent moisture conditions) in the flood generation processes (Berghuijs et al., 2019; Cao et al., 2019; Ivancic & Shaw, 2015; Li et al., 2009; Radatz et al., 2012; Tramblay et al., 2010).
2. The probability of floods driven by extreme precipitation (PF_{EP}) varies between 0.55 and 0.7 at the four gage stations of the GRB. We find that the PF_{EP} declines as the size of the river basin increases, which might be associated with the spatial distribution of extreme precipitation in the basin. At all the four locations in the GRB, more than 80% of extreme precipitation events that caused floods, occurred on wet antecedent moisture conditions. Moreover, more than 50% of extreme precipitation events that did not cause floods occurred on non-wet antecedent moisture conditions during the observed period (1955–2016) period.
3. The frequency of extreme precipitation and flood events is projected to increase at all four locations of the GRB under the future climate (2071–2100). However, the rise in extreme precipitation and flood events is higher under RCP 8.5 in comparison to RCP 2.6. Here it is important to note that we did not consider the projected changes in land use under the future climate, which may also considerably influence the floods in GRB.
4. PF_{EP} is projected to increase under the future climate in comparison to the historical period at all the four gage stations of GRB. The frequency of extreme precipitation events is projected to rise by two folds or more at all the four locations in Godavari basin, and the increased frequency of floods under the future climate will largely be driven by the rise in the extreme precipitation events rather than wet antecedent moisture conditions. Our results show that climate change mitigation can be beneficial in reducing the frequency of floods in GRB. However, the observed and projected changes in the floods can be influenced by both anthropogenic (land use/land cover and reservoir operations) and climatic factors (extreme precipitation, initial moisture condition, and interstorm duration) that need to be evaluated in the future work.

Acknowledgments
All the data used this study are available from India Meteorological Department (www.imd.gov.in), India-WRIS (http://www.india-wris.nrsc.gov.in), and CMIP5 (https://esgf-node.llnl.gov/projects/cmip5/). Authors acknowledge the funding from Ministry of Human Resources Development (MHRD), National Water Mission, and Ministry of Earth Sciences (MoES) under the Monsoon Mission II. The first author appreciate comments and suggestions from Dennis Lettenmaier. All the data used in this study are being uploaded for public use on GitHub.

References

Ali, H., & Mishra, V. (2017). Contrasting response of rainfall extremes to increase in surface air and dewpoint temperatures at urban locations in India. *Scientific Reports*, *7*(1), 1–15. https://doi.org/10.1038/s41598-017-01306-1

Ali, H., & Mishra, V. (2018). Increase in Subdaily Precipitation Extremes in India Under 1.5 and 2.0 °C Warming Worlds. *Geophysical Research Letters*, *45*, 6972–6982. https://doi.org/10.1029/2018GL078689

Ali, H., Modi, P., & Mishra, V. (2019). Increased flood risk in Indian sub-continent under the warming climate. *Weather and Climate Extremes*, *25*(May), 100212. https://doi.org/10.1016/j.wace.2019.100212

Arnell, N. W., & Gosling, S. N. (2016). The impacts of climate change on river flood risk at the global scale. *Climatic Change*, *134*(3), 387–401 . https://doi.org/10.1007/s10584-014-1084-5

Ashfaq, M., Rastogi, D., Mei, R., Touma, D., & Ruby Leung, L. (2017). Sources of errors in the simulation of south Asian summer monsoon in the CMIP5 GCMs. *Climate Dynamics*, *49*(1–2), 193–223. https://doi.org/10.1007/s00382-016-3337-7

Asoka, A., Wada, Y., Fishman, R., & Mishra, V. (2018). Strong Linkage Between Precipitation Intensity and Monsoon Season Groundwater Recharge in India. *Geophysical Research Letters*, *45*, 5536–5544. https://doi.org/10.1029/2018GL078466

Asouti, E., & Fuller, D. Q. (2008). Trees and woodlands of South India: Archaeological perspectives. Trees and woodlands of South India: Archaeological perspectives. Retrieved from https://www.cabdirect.org/cabdirect/abstract/20083223781

Berghuijs, W. R., Harrigan, S., Molnar, P., Slater, L. J., & Kirchner, J. W. (2019). The Relative Importance of Different Flood-Generating Mechanisms Across Europe. *Water Resources Research*, *55*(6), 4582–4593. https://doi.org/10.1029/2019WR024841

Bhattachaiyya, N. N., & Bora, A. K. (1997). Floods of the brahmaputra river in india. *Water International*, *22*(4), 222–229. https://doi.org/10.1080/02508069708686709

Blöschl, G., Nester, T., Komma, J., Parajka, J., & Perdigão, R. (2013). The June 2013 flood in the Upper Danube Basin, and comparisons with the 2002, 1954 and 1899 floods. *Hydrology and Earth System Sciences*, *17*(12), 5197–5212. https://doi.org/10.5194/hess-17-5197-2013

Blöschl, G., Gaál, L., Hall, J., Kiss, A., Komma, J., Nester, T., et al. (2015). Increasing river floods: Fiction or reality? *Wiley Interdisciplinary Reviews Water*, *2*(4), 329–344. https://doi.org/10.1002/wat2.1079

Camici, S., Tarpanelli, A., Brocca, L., Melone, F., & Moramarco, T. (2011). Design soil moisture estimation by comparing continuous and storm-based rainfall-runoff modeling. *Water Resources Research*, *47*, W05527. https://doi.org/10.1029/2010WR009298

Cao, Q., Mehran, A., Ralph, F. M., & Lettenmaier, D. P. (2019). The role of hydrological initial conditions on Atmospheric River floods in the Russian River basin. *Journal of Hydrometeorology*, 1–60. https://doi.org/10.1175/JHM-D-19-0030.1

Cea, L., & Fraga, I. (2018). Incorporating Antecedent Moisture Conditions and Intraevent Variability of Rainfall on Flood Frequency Analysis in Poorly Gauged Basins. *Water Resources Research*, *54*, 8774–8791. https://doi.org/10.1029/2018WR023194

Cherkauer, K. A., Bowling, L. C., & Lettenmaier, D. P. (2003). Variable infiltration capacity cold land process model updates. *Global and Planetary Change*, *38*(1–2), 151–159. https://doi.org/10.1016/S0921-8181(03)00025-0

Cherkauer, K. A., & Lettenmaier, D. P. (1999). Layer, 104.

Deshpande, N. R., Kothawale, D. R., & Kulkarni, A. (2016). Changes in climate extremes over major river basins of India. *International Journal of Climatology*, *36*(14), 4548–4559. https://doi.org/10.1002/joc.4651

Dhar, O. N., & Nandargi, S. (2000). A study of floods in the Brahmaputra basin in India. *International Journal of Climatology*, *20*(7), 771–781 . https://doi.org/10.1002/1097-0088(20000615)20:7<771::AID-JOC518>3.0.CO;2-Z

Dhar, O. N., & Nandargi, S. (2003). Hydrometeorological Aspects of Floods in India. *Natural Hazards*, *28*(1), 1–33. https://doi.org/10.1023/A:1021199714487

Dhar, O. N., Rakhecha, P. R., Mandal, B. N., & Sangam, R. B. (1981). The rainstorm which caused the morvi dam disaster in august 1979. *Hydrological Sciences Bulletin*, *26*(1), 71–81. https://doi.org/10.1080/02626668109490862

Gao, H., Tang, Q., Shi, X., Zhu, C., Bohn, T., & Su, F. (2009). Water Budget Record from Variable Infiltration Capacity (VIC) Model Algorithm Theoretical Basis Document. Rapport - Version 1.2, (Vic), 57.

Geert Jan van Oldenborgh, F. E. L. O., Haustein, K., & AchutaRao, K. (2016). The Heavy Precipitation Event Of December 2015 In Chennai, India. *Bulletin of the American Meteorological Society*, *97*(12), 145. https://doi.org/10.1175/BAMS-D-16-0149

Goswami, B. N., Venugopal, V., Sengupta, D., Madhusoodanan, M. S., & Xavier, P. K. (2006). Earth by comets and meteorites. Further studies of these objects may elucidate whether their composition and membrane-like structures were important building blocks for the origin of life. *Science*, *314*(December), 1442–1445. https://doi.org/10.1126/science.1132027

Gulf News. (2018). Kerala flood live: Hundreds dead, hundreds of thousands homeless, clean-up drive starts|GulfNews.com. Retrieved from https://gulfnews.com/news/asia/india/kerala-flood-livehundreds-dead-hundreds-of-thousands-homeless-clean-up-drive-starts1.2268422

Gunnell, Y., Anupama, K., & Sultan, B. (2007). Response of the South Indian runoff-harvesting civilization to northeast monsoon rainfall variability during the last 2000 years: Instrumental records and indirect evidence. *Holocene*, *17*(2), 207–215. https://doi.org/10.1177/0959683607075835

Gupta, A. K., & Nair, S. S. (2010). Urban floods in Bangalore and Chennai: Risk management challenges and lessons for sustainable urban ecology, (October 2016). *Current Science (Bangalore)*, *100*(11), 1638–1645.

Hansen, M. C., Defries, R. S., Townshend, J. R. G., & Sohlberg, R. (2000). International Journal of Remote Sensing Global land cover classification at 1 km spatial resolution using a classification tree approach Global land cover classii cation at 1 km spatial resolution using a classii cation tree approach. *International Journal of Remote Sensing*, *21*(7), 1331–1364. https://doi.org/10.1080/014311600210209

Hempel, S., Frieler, K.,Warszawski, L., Schewe, J., & Piontek, F. (2013). A trend-preserving bias correction–the ISI-MIP approach. *Earth System Dynamics*, *4*(2), 219–236. https://doi.org/10.5194/esd-4-219-2013

Hirabayashi, Y., Mahendran, R., Koirala, S., Konoshima, L., Yamazaki, D., Watanabe, S., et al. (2013). Global flood risk under climate change. *Nature Climate Change*, *3*(9), 816–821. https://doi.org/10.1038/nclimate1911

Ivancic, T. J., & Shaw, S. B. (2015). Examining why trends in very heavy precipitation should not be mistaken for trends in very high river discharge. *Climatic Change*, *133*(4), 681–693. https://doi.org/10.1007/s10584-015-1476-1

Jena, P. P., Chatterjee, C., Pradhan, G., & Mishra, A. (2014). Are recent frequent high floods in Mahanadi basin in eastern India due to increase in extreme rainfalls? *Journal of Hydrology*, *517*, 847–862. https://doi.org/10.1016/j.jhydrol.2014.06.021

Kale, V. (2012). On the link between extreme floods and excess monsoon epochs in South Asia. *Climate Dynamics*, *39*(5), 1107–1122. https://doi.org/10.1007/s00382-011-1251-6

Kumar, S. (2013). Rapidly assessing flood damage in Uttarakhand, India. Retrieved from from http://documents.worldbank.org/curated/en/724891468188654600/Rapidlyassessing-flood-damage-in-Uttarakhand-India.

Kundzewicz, Z. W., Kanae, S., Seneviratne, S. I., Handmer, J., Nicholls, N., Peduzzi, P., et al. (2014). Flood risk and climate change: Global and regional perspectives flood risk and climate change: Global and regional perspectives. *Hydrological Sciences Journal – Journal Des Sciences Hydrologiques*, *59*(1), 1–28. https://doi.org/10.1080/02626667.2013.857411

Li, H., Luo, L., Wood, E. F., & Schaake, J. (2009). The role of initial conditions and forcing uncertainties in seasonal hydrologic forecasting. *Journal of Geophysical Research*, *114*, D04114. https://doi.org/10.1029/2008JD010969

Liang, X., Lettenmaier, D. P., Wood, E. F., & Burges, S. J. (1994). A simple hydrologically based model of land surface water and energy fluxes for general circulation models. *Journal of Geophysical Research*, *99*(D7), 14,415. https://doi.org/10.1029/94JD00483

Liang, X., Wood, E. F., & Lettenmaier, D. P. (1996). Surface soil moisture parameterization of the VIC-2L model: Evaluation and modification. *Global and Planetary Change*, *13*(1–4), 195–206. https://doi.org/10.1016/0921-8181(95)00046-1

Lohmann, D., Nolte-Holube, R., & Raschke, E. (1996). A large-scale horizontal routing model to be coupled to land surface parametrization schemes. *Tellus Series A: Dynamic Meteorology and Oceanography*, *48*(5), 708–721. https://doi.org/10.3402/tellusa.v48i5.12200

Lohmann, D., Raschke, E., Nijssen, B., & Lettenmaier, D. P. (1998). Regional scale hydrology: II. Application of the VIC-2L model to the Weser River, Germany. *Hydrological Sciences Journal*, *43*(1), 143–158. https://doi.org/10.1080/02626669809492108

Mann, H. B. (1945). Nonparametric Tests Against Trend Author (s): Henry B. Mann Published by: The Econometric Society Stable URL: https://www.jstor.org/stable/1907187 REFERENCES Linked references are available on JSTOR for this article: You may need to log in to JSTOR, 13(3), 245–259.

Massari, C., Brocca, L., Moramarco, T., Tramblay, Y., & Lescot, J. D. (2014). Advances in Water Resources Potential of soil moisture observations in flood modelling: Estimating initial conditions and correcting rainfall. *Advances in Water Resources*, *74*, 44–53. https://doi.org/10.1016/j.advwatres.2014.08.004

Maurer, E. P., Wood, A. W., Adam, J. C., Lettenmaier, D. P., & Nijssen, B. (2002). A Long-Term Hydrologically-Based Data Set of Land Surface Fluxes and States for the Conterminous {United States}. *Journal of Climate*, *15*(22), 3237–3251. https://doi.org/10.1175/1520-0442(2002)015<3237:ALTHBD>2.0.CO;2

Merz, R., & Blöschl, G. (2009). A regional analysis of event runoff coefficients with respect to climate and catchment characteristics in Austria. *Water Resources Research*, *45*, W01405. https://doi.org/10.1029/2008WR007163

Milly, P. C. D., Wetherald, R. T., Dunne, K. A., & Delworth, T. L. (2002). Increasing risk of great foods in a changing climate. *Nature*, *415*(6871), 514–517. https://doi.org/10.1038/415514a

Min, S., Zhang, X., Zwiers, F. W., & Hegerl, G. C. (2011). Human contribution to more-intense precipitation extremes. *Nature*, *470*(7334), 378–381. https://doi.org/10.1038/nature09763

Mirza, M. M. Q. (2011). Climate change, flooding in South Asia and implications. *Regional Environmental Change*, *11*(1), 95–107. https://doi.org/10.1007/s10113-010-0184-7

Mishra, V., Aaadhar, S., Shah, H., Kumar, R., Pattanaik, D. R., & Tiwari, A. D. (2018). The Kerala flood of 2018: Combined impact of extreme rainfall and reservoir storage. Hydrology and Earth System Sciences Discussions, (September), 1–13. https://doi.org/10.5194/hess-2018-480

Mishra, V., Dominguez, F., & Lettenmaier, D. P. (2012). Urban precipitation extremes: How reliable are regional climate models? *Geophysical Research Letters*, *39*, L03407. https://doi.org/10.1029/2011GL050658

Mishra, V., & Shah, H. L. (2018). Hydroclimatological Perspective of the Kerala Flood of 2018. *Journal of the Geological Society of India*, *92*(5), 645–650. https://doi.org/10.1007/s12594-018-1079-3

Mishra, V., Shah, R., Azhar, S., Shah, H., Modi, P., & Kumar, R. (2018). Reconstruction of droughts in India using multiple land-surface models (1951-2015). *Hydrology and Earth System Sciences*, *22*(4), 2269–2284.

Mohapatra, P. K., & Singh, R. D. (2003). Flood management in India. *Natural Hazards*, *28*(1), 131–143. https://doi.org/10.1023/A:1021178000374

Moriasi, D. N., Arnold, J. G., van Liew, M. W., Bingner, R. L., Harmel, R. D., & Veith, T. L. (2007). Model evaluation guidelines for systematic quantification of accuracy in watershed simulations. *Transactions of the ASABE*, *50*(3), 885–900. https://doi.org/10.13031/2013.23153

Moss, R. H., Edmonds, J. A., Hibbard, K. A., Manning, M. R., Rose, S. K., van Vuuren, D. P., et al. (2010). The next generation of scenarios for climate change research and assessment. *Nature*, *463*(7282), 747–756. https://doi.org/10.1038/nature08823

Mukherjee, S., Aadhar, S., Stone, D., & Mishra, V. (2018). Increase in extreme precipitation events under anthropogenic warming in India. *Weather and Climate Extremes*, *20*(March), 45–53. https://doi.org/10.1016/j.wace.2018.03.005

Nageswara Rao, G. (2001). Occurrence of heavy rainfall around the confluence line in monsoon disturbances and its importance in causing floods. *Proceedings of the Indian Academy of Sciences, Earth and Planetary Sciences*, *110*(1), 87–94.

Nash, J. E., & Sutcliffe, J. V. (1970). River flow forecasting through conceptual models part I — A discussion of principles. *Journal of Hydrology*, *10*(3), 282–290. https://doi.org/https://doi.org/10.1016/0022-1694(70)90255-6

Pai, D. S., Sridhar, L., Badwaik, M. R., & Rajeevan, M. (2015). Analysis of the daily rainfall events over India using a new long period (1901–2010) high resolution (0.25° × 0.25°) gridded rainfall data set. *Climate Dynamics*, *45*(3–4), 755–776. https://doi.org/10.1007/s00382-014-2307-1

Pilgrim, D. H., Cordery, I., & Baron, B. C. (1982). Effects of catchment size on runoff relationships. *Journal of Hydrology*, *58*(3–4), 205–221. https://doi.org/10.1016/0022-1694(82)90035-X

Radatz, T. F., Thompson, A. M., & Madison, F. W. (2012). Soil moisture and rainfall intensity thresholds for runoff generation in southwestern Wisconsin agricultural watersheds. *Hydrological Processes*, *27*(25), 3521–3534. https://doi.org/10.1002/hyp

Rakhecha, P., & Singh, V. (2017). Enveloping Curves for the Highest Floods of River basins in India. *International Journal of Hydrology*, *1*(3), 79–84. https://doi.org/10.15406/ijh.2017.01.00015

Rakhecha, P. R. (2002). Highest floods in India. IAHS PUBLICATION, 167-172

Roxy, M. K., Ghosh, S., Pathak, A., Athulya, R., Mujumdar, M., Murtugudde, R., et al. (2017). A threefold rise in widespread extreme rain events over central India. *Nature Communications*, *8*(1), 1–11. https://doi.org/10.1038/s41467-017-00744-9

Saharia, M., Kirstetter, P., Vergara, H., & Gourley, J. J. (2017). Characterization of floods in the United States. *Journal of Hydrology*, *548*, 524–535. https://doi.org/10.1016/j.jhydrol.2017.03.010

Sen, P. K. (1968). Journal of the American Statistical Estimates of the Regression Coefficient Based on Kendall ' s Tau, (April 2013), 37–41.

Shah, H. L., & Mishra, V. (2016). Hydrologic Changes in Indian Subcontinental River Basins (1901–2012). *Journal of Hydrometeorology*, *17*(10), 2667–2687. https://doi.org/10.1175/jhm-d-15-0231.1

Shah, H. L., Zhou, T., Huang, M., & Mishra, V. (2019). Strong Influence of Irrigation on Water Budget and Land Surface Temperature in Indian Subcontinental River Basins. *Journal of Geophysical Research: Atmospheres*, *124*, 1449–1462. https://doi.org/10.1029/2018JD029132

Sharma, A., Wasko, C., & Lettenmaier, D. P. (2018). If Precipitation Extremes Are Increasing, Why Aren't Floods? *Water Resources Research*, *54*, 8545–8551. https://doi.org/10.1029/2018WR023749

Shepard, D. S. (1984). Computer Mapping: The SYMAP Interpolation Algorithm. *Spatial Statistics and Models*, 133–145. https://doi.org/10.1007/978-94-017-3048-8_7

Sinha, R., Bapalu, G. V., Singh, L. K., & Rath, B. (2008). Flood risk analysis in the Kosi river basin, north Bihar using multi-parametric approach of Analytical Hierarchy Process (AHP). *Journal of the Indian Society of Remote Sensing*, *36*(4), 335–349. https://doi.org/10.1007/s12524-008-0034-y

Slater, L. J., & Wilby, R. L. (2017). Measuring the changing pulse of rivers. *Science*, *357*, 552–522. https://doi.org/10.1126/science.aao2441

Smith, J. A., Villarini, G., Wright, D. B., & Krajewski, W. (2013). Extreme flood response: The June 2008 flooding in Iowa, (June 2008). *Journal of Hydrometeorology*, *14*(6), 1810–1825. https://doi.org/10.1175/JHM-D-12-0191.1

Srivastava, A. K., Rajeevan, M., & Kshirsagar, S. R. (2009). Development of a high resolution daily gridded temperature data set (1969-2005) for the Indian region. *Atmospheric Science Letters*, *10*, 249–254. https://doi.org/10.1002/asl.232

Sudheer, K. P., Murty Bhallamudi, S., Narasimhan, B., Thomas, J., Bindhu, V. M., Vema, V., & Kurian, C. (2019). Role of dams on the floods of August 2018 in Periyar River Basin, Kerala. *Current Science*, *116*(5), 780–794. https://doi.org/10.18520/cs/v116/i5/780-794

Taylor, K. E., Stouffer, R. J., & Meehl, G. A. (2012). An overview of CMIP5 and the experiment design. *Bulletin of the American Meteorological Society*, *93*(4), 485–498. https://doi.org/10.1175/BAMS-D-11-00094.1

Terrell, G. R., & Scott, D. W. (1992). Variable kernel density estimation. *The Annals of Statistics*, *20*(3), 1236–1265.

Tramblay, Y., Bouvier, C., Martin, C., Didon-lescot, J., Todorovik, D., & Domergue, J. (2010). Assessment of initial soil moisture conditions for event-based rainfall – runoff modelling. *Journal of Hydrology*, *387*(3–4), 176–187. https://doi.org/10.1016/j.jhydrol.2010.04.006

Trenberth, K. E., Dai, A., Rasmussen, R. M., & Parsons, D. B. (2003). The changing character of precipitation. *Bulletin of the American Meteorological Society*, *84*, 1205–1217.

Wasko, C., & Sharma, A. (2015). Steeper temporal distribution of rain intensity at higher temperatures within Australian storms. *Nature Geoscience*, *8*(July), 527–529. https://doi.org/10.1038/ngeo2456

Wasko, C., & Sharma, A. (2017). Global assessment of flood and storm extremes with increased temperatures. *Scientific Reports*, *7*(1), 7945. https://doi.org/10.1038/s41598-017-08481-1

Westra, S., Alexander, L. V., & Zwiers, F. W. (2013). Global Increasing Trends in Annual Maximum Daily Precipitation. *Journal of Climate*, *26*(2005), 3904–3918. https://doi.org/10.1175/JCLI-D-12-00502.1

Yue, S., Pilon, P., Phinney, B., & Cavadias, G. (2002). The influence of autocorrelation on the ability to detect trend in hydrological series. *Hydrological Processes*, *16*(9), 1807–1829. https://doi.org/10.1002/hyp.1095